Proc. Natl. Acad. Sci. USA
Vol. 90, pp. 6199–6202, July 1993
Biochemistry

The 3′-terminal end (NCCA) of tRNA determines the structure and stability of the aminoacyl acceptor stem

(RNA synthesis/RNA structure/^{1}H NMR/aminoacyl-tRNA synthetase)

STEFAN LIMMER, HANS-PETER HOFMANN, GÜNTHER OTT, AND MATHIAS SPRINZL*

Laboratorium für Biochemie, Universität Bayreuth, Postfach 10 12 51, W-8580 Bayreuth, Federal Republic of Germany

Communicated by Paul Schimmel, March 16, 1993

ABSTRACT **We have done a systematic study on the contribution of the single-stranded NCCA end (where N is any nucleotide) to the stability of the aminoacyl stem of tRNA. A 7-bp RNA duplex with the single-strand ACCA 3′ terminus derived from the aminoacyl stem of *Escherichia coli* tRNA^{Ala} and several chemically synthesized sequence variants are characterized by proton NMR and thermodynamic parameters. The single-stranded 3′ terminus noticeably stabilizes the duplex in a sequence-dependent manner. Though the largest contribution to the stability gain due to the ACCA end is provided by the first dangling 3′ nucleotide, the influence of even the fourth nucleotide is measurable. The nature of the N73 discriminator base influences the stem structure and stability, which may be important for the recognition of tRNA by aminoacyl-tRNA synthetase. The stepwise attachment of the nucleotides to the 3′ tail improves the stacking of the unpaired bases over the helix stem. Hence, the ACCA end appears to be structured. Replacing Mg^{2+} with Mn^{2+} causes broadening of certain imino proton peaks in the NMR spectrum, indicating a specific divalent metal ion binding site in the vicinity of the major identity element of the duplex (G3–U70) that is required for its recognition by the Ala-tRNA synthetase.**

tRNAs possess a single-stranded 3′ terminus consisting of 4 nt, the last three of which invariably are CCA. The nonpaired nucleotide preceding the ubiquitous CCA terminus, the so-called discriminator base (1), can be any one of the 4 nt A, G, U, or C. If the occurrence of the 4 nt in positions 1, 72, and 73 is analyzed in the available tRNA sequences (2), the following conclusions can be derived (Fig. 1): (*i*) There is a preference for purine in position 1 (86%) with a clear prevalence of guanosine (76%) that is matched by a corresponding preference for pyrimidines (86.5%; 70% cytidine) in position 72; (*ii*) position 73 is preferentially occupied by purines (85%; with 62% being adenosine). Hence, the most frequent configuration consists of a G·C bp between positions 1 and 72 with a nonpaired adenosine at position 73 that is presumably stacked upon the base-paired pyrimidine at position 72. This corresponds to the arrangement of the terminal base pair and nonpaired 3′ nucleotide, which is most stable according to the duplex-stability-prediction rules derived from systematic thermodynamic studies by Turner and coworkers (3, 4).

The duplexes studied in the present work (Fig. 2) can be regarded as representative examples of tRNA acceptor stems with single-stranded 3′ termini. They are derived from the acceptor arm of the *Escherichia coli* alanine-specific tRNA and bear homology to the "microhelix^{Ala}," which has been shown to be enzymatically aminoacylated with alanine (5, 6).

Though there are convincing data proving the favorable effect of dangling 3′ ends on duplex stability, there has been no investigation concerning the influence of the further nonpaired bases of the NCCA end of tRNA (where N is any nucleotide). Therefore, we studied the duplex in its full-length form (Fig. 2) and variants with gradually truncated single-stranded 3′ ends and arrived finally at the duplex without nonpaired nucleotides. Moreover, duplexes with altered single-strand sequences and modified helix stems have been investigated for comparison.

From studies of yeast tRNA^{Phe}, it is known that there are several specifically bound magnesium ions that stabilize the tertiary structure and could have a functional role (7). One of these binding sites is localized in the acceptor stem; hence, we wanted to determine whether one could be detected in the acceptor-stem-derived microhelices.

MATERIALS AND METHODS

RNA oligonucleotides were synthesized chemically on a Gene Assembler Plus (Pharmacia) using H-phosphonate synthones according to a procedure described previously (8). The 5′ and 2′ OH groups of ribose were protected by 4,4′-dimethoxytrityl and *tert*-butyldimethylsilyl protecting groups, respectively. Protection of the exocyclic amines in adenine and guanine was achieved by dimethylaminomethylene protection groups (8). The oligonucleotides were purified by HPLC on a Vydac C_4 column. The RNA synthones were purchased from DIAGEN (Düsseldorf, F.R.G.). Single-strand RNA concentrations for NMR measurements were typically 0.5–1.5 mM. The total volume of the samples was 0.5 ml. The buffer contained 100 mM NaCl and 10 mM sodium phosphate (pH 6.5). Where indicated, $MgCl_2$ (5–7.5 mM) was added.

The NMR spectra were determined on a Bruker AM 500 spectrometer operating at a proton resonance frequency of 500 MHz. To suppress the strong water signal, the 1–3–3–1 pulse sequence according to Hore (9) was applied. Chemical shifts are referenced to internal 2,2-dimethyl-2-silapentane-5-sulfonate.

The UV absorbance measurements were carried out on a DU-8 spectrophotometer (Beckman) equipped with a variable-temperature unit. Absorbance at 260 nm was registered while heating 1-ml samples at a rate of 1 K/min. Single-strand RNA concentrations were 3 μM in all cases, and the buffer was the same as in the NMR samples. Thermodynamic parameters were determined on the basis of the two-state model from the temperature dependence of the equilibrium constant (10).

RESULTS

Chemical-Shift Alterations of the Imino Proton Resonances with the Length of the Single-Stranded 3′ Terminus. One-dimensional proton NMR in aqueous solution was employed to monitor the formation of secondary structures of the RNA

The publication costs of this article were defrayed in part by page charge payment. This article must therefore be hereby marked "*advertisement*" in accordance with 18 U.S.C. §1734 solely to indicate this fact.

*To whom reprint requests should be addressed.

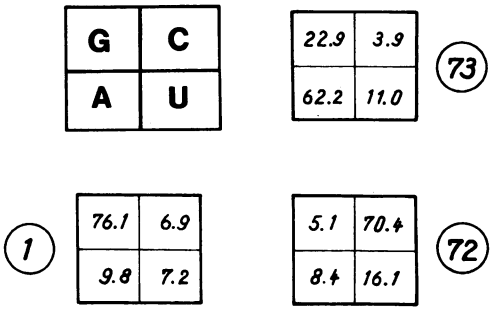

FIG. 1. Occurrence of the nucleotides A, G, U, and C in positions 1, 72, and 73 (circled) of tRNAs (2). The relative frequencies (in percent) of the nucleotides in the respective position are given in the boxes corresponding to the scheme at the upper left.

helices. Fig. 3 depicts the down-field regions of the proton NMR spectra of the RNA duplex shown in Fig. 2 (18-mer) along with its variants possessing successively truncated single-stranded 3′ ends, denoted in the following as 17-mer (spectrum d), 16-mer (spectrum c), 15-mer (spectrum b), and 14-mer (spectrum a). The assignment of the lines (Fig. 3, spectrum a) was achieved by nuclear Overhauser effect experiments, evaluation of the spectral changes upon sequence variations, and replacement of the G·U base pair by I·U, I·C, or G·C. The U imino proton signal of the A·U base pair at position 7 remained invisible at 3°C due to the high base-pair opening rate ("fraying") and hence increased proton exchange. The lines corresponding to the imino protons of the G·U wobble pair can be identified by their exceptionally strong mutual nuclear Overhauser effects.

The effect of the stepwise addition of nonpaired nucleotides onto the first (G·C) base pair of the 14-mer duplex is documented in Fig. 4, where the up-field shift of the imino protons of bp 1–3 is plotted versus the number of nonpaired dangling 3′ nucleotides. The most dramatic up-field shift is observed upon the addition of the first 3′ adenosine. The imino proton resonance of bp 1 was most strongly influenced, yet the peak of bp 2 was also considerably shifted, as was the guanosine imino resonance of bp 3—though to a much lesser extent. Surprisingly, further extension of the single-stranded 3′ end was clearly sensed by the imino protons, especially those of bp 1 and 2. Even the fourth nucleotide (adenosine) of the 3′ terminus gave rise to a measurable up-field-shift increment. When the spectra of the duplexes possessing dangling 3′ ends (Fig. 3 *b–e*) were compared with that of the 14-mer (Fig. 3*a*), another significant effect was seen. The linewidth of the imino proton of bp 1 was markedly reduced in the presence of a dangling 3′ nucleotide, indicating a reduction of the proton exchange rate and reflecting the stabilization of bp 1 (3, 4).

Stability of the Duplexes and Their Individual Base Pairs. The linewidth of exchangeable imino protons is determined mainly by their exchange rates with water. More quantitatively, the excess linewidth at half-maximum height, $\Delta\nu_{ex}$, due to exchange broadening (i.e., the residual linewidth after subtraction of the linewidth contribution in absence of exchange) is related to the proton exchange rate k_{ex} via $k_{ex} = \pi\Delta\nu_{ex}$. A plot of the excess linewidths versus reciprocal temperature usually yields reasonably good straight lines whose slopes provide activation enthalpies for the exchange

FIG. 2. RNA duplex (18-mer) derived from the acceptor stem of *E. coli* $tRNA^{Ala}$. The numbering denotes the base-pair positions.

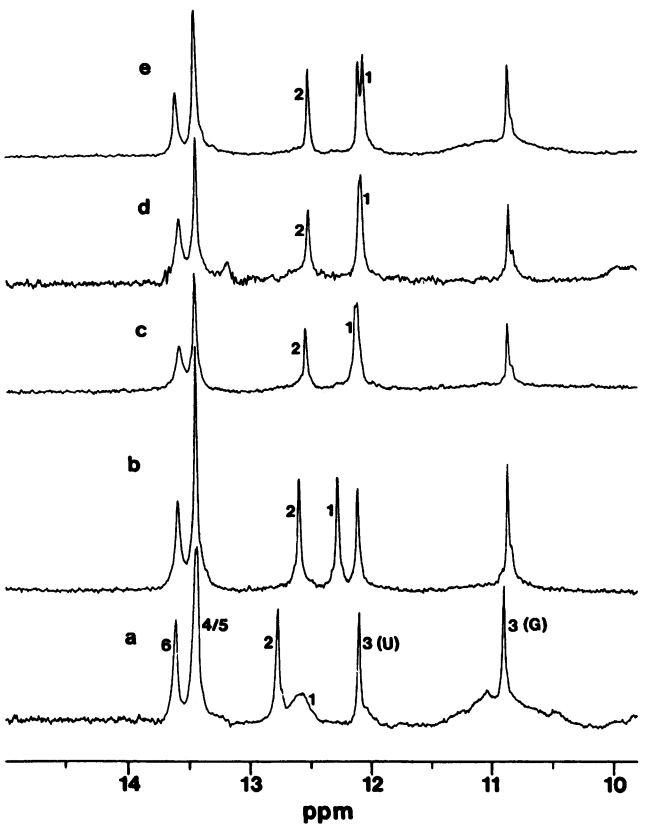

FIG. 3. Down-field part of the proton NMR spectra of different RNA duplex variants derived from the original structure given in Fig. 2. Spectra: a, 14-mer; b, 15-mer; c, 16-mer; d, 17-mer; e, 18-mer. The assignment of the peaks to the corresponding base pairs is given in spectrum a, in all the other spectra only the peaks due to bp 1 and 2 are indicated.

process. Such an analysis showed an increase in the activation enthalpy for both the first and the second base pairs after attachment of dangling 3′ bases. Moreover, the activation enthalpy for the first base pair was distinctly lower than that for the second base pair (typically by ≈100 kJ/mol).

To characterize the overall stability of the duplexes, the optical melting curves were recorded for all oligonucleotides. The thermodynamic parameters melting temperature (T_m), Gibbs free energy of duplex formation at 37°C (ΔG^0), enthalpy of duplex formation (ΔH^0), and entropy of duplex formation (ΔS^0) for various oligonucleotides were compiled along with the activation enthalpies for the exchange of the imino proton of bp 2, $\Delta H_a^{(2)}$ (Table 1). The bp 2 was selected since (*i*) its imino proton peak was well-separated from all other imino resonances in the investigated duplexes, (*ii*) it was sufficiently stable even in the duplex without dangling end and was still sufficiently close to the end of the helical stem to sense the influence of the single-stranded region, and (*iii*) finally, it was a neighbor to the G·U base pair at position 3, which is an identity element in *E. coli* $tRNA^{Ala}$ (5).

There was a good agreement in the course of $\Delta\delta$,$\Delta H_a^{(2)}$, ΔG^0, and T_m with increasing single-strand length (Fig. 4 and Table 1). All data demonstrated the stabilizing effect of the single-stranded 3′ end with the largest contribution provided by the 3′ adenosine that is next to the G·C base pair. Additional nonpaired nucleotides up to position 4 further stabilized the duplex although their individual contributions gradually decreased.

Alterations of the sequence of the single-stranded terminus to 3′-ACCC and 3′-AUUA caused reductions of the duplex stability, as did the inversion of the first base pair from G·C to C·G. Likewise, attachment of the 3′-ACCA terminus to the

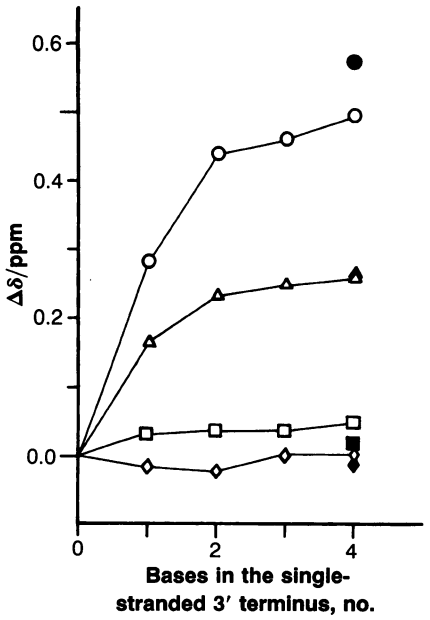

FIG. 4. Up-field shift of the imino proton resonances of bp 1 (○), 2 (△), 3G (□), and 3U (◇) upon stepwise attachment of dangling 3′ nucleotides onto the bp 1 of the 14-mer at 4°C. For comparison, the up-field shifts are given for the variants with an I·U base pair at position 3 (solid symbols).

opposite end of the duplex stem (i.e., at the adenosine of the A·U base pair at position 7) gave rise to a stabilization increment, $\Delta\Delta G^0$, of only 2 kJ/mol relative to the 14-mer (Table 2). This was considerably lower than the $\Delta\Delta G^0$ of 3.3 kJ/mol expected from the theoretical prediction rules (4) for adding only a single unpaired adenosine. The theoretical increment system was based on measurements in 1 M NaCl, whereas our studies were performed with 0.1 M NaCl.

Replacing the G·U base pair at position 3 with I·U (inosine lacks the 2-amino group compared to guanosine) produced an increase in ΔG^0 of 8.6 kJ/mol for the 14-mer and 4.4 kJ/mol for the 18-mer. For the I·U duplex, the gain in overall thermodynamic stability upon attachment of the ACCA 3′ terminus was −14.7 kJ/mol.

Binding of Divalent Cations. Addition of Mg^{2+} in millimolar concentrations to the duplex RNA solutions caused small line-shift changes up to 0.04 ppm. These were different in magnitude and sign for the individual base pairs for the duplexes with and without an ACCA end. To check whether these small differences in chemical shift of NH resonances are related to variations in divalent ion binding affinity along

Table 1. Thermodynamic parameters for duplex formation and activation enthalpies for imino proton exchange of bp 2

Duplex	$\Delta H_a^{(2)}$, kJ/mol	T_m, °C	ΔG^0, kJ/mol	ΔH^0, kJ/mol	ΔS^0, J/mol K
14-mer (without dangling end)	223	35.9	−33.4	−314.6	−907
15-mer (3′-A)	266	43.3	−41.0	−336.4	−952
16-mer (3′-CA)	256	44.6	−41.5	−300.4	−835
17-mer (3′-CCA)	295	45.6	−43.3	−328.0	−918
18-mer (3′-ACCA)	301	45.9	−43.9	−339.7	−954
18-mer/5 mM $MgCl_2$	338	50.8	−48.9	−340.6	−941

T_m, melting temperature; $\Delta H_a^{(2)}$, activation enthalpy for the exchange of the G-N1H of bp 2 with water; ΔG^0, Gibbs free energy for duplex formation at 37°C; ΔH^0, enthalpy change for duplex formation; ΔS^0, entropy change for duplex formation. Typical experimental errors: ±0.5°C, for T_m; ±5–10%, for ΔH^0 and ΔS^0; ±2%, for ΔG^0; ±5% for $\Delta H_a^{(2)}$. Single-strand concentrations in the melting curve analyses were always 3 μM.

Table 2. Gibbs free energies, melting temperatures, and activation enthalpies for bp-2 imino proton exchange for several duplex variants

Duplex	$\Delta H_a^{(2)}$, kJ/mol	T_m, °C	ΔG^0, kJ/mol
3′-ACCA at inverted bp 1	ND	39.7	−37.3
3′-ACCC at bp 1	ND	41.6	−38.6
3′-AUUA at bp 1	182	44.8	−42.2
3′-ACCA at bp 7	163	38.1	−35.4
14-mer/I·U at position 3	ND	28.1	−24.8
18-mer/I·U at position 3	268	41.5	−39.5

ND, not determinable; T_m, melting temperature. Other abbreviations are as in Table 1.

the duplex, Mg^{2+} was replaced by paramagnetic Mn^{2+}. Mn^{2+} can replace Mg^{2+} in many cases without hampering the specific functions of RNA (11, 12). The imino resonance regions of the proton NMR spectra of the 14-mer and the 18-mer before and after addition of $MnCl_2$, respectively, are presented in Fig. 5. For both duplexes, the imino lines originating from bp 4–6 did not show noticeable broadening upon addition of paramagnetic Mn^{2+}, whereas the imino proton signals from bp 2 (excess linewidth of 51 Hz for the 14-mer and 43 Hz for the 18-mer) and bp 3, and to a lesser extent also that from bp 1 (excess linewidth about 16 Hz for the 14-mer), were severely broadened. For the 14-mer, it was seen that the broadening of the bp-3 uridine imino peak (38 Hz) is more pronounced than that of its guanosine imino proton (10 Hz). A similar statement is not possible for the 18-mer due to the superposition of the uridine imino proton peak of bp 3 and the guanosine imino proton resonance of bp 1 (excess linewidth for the guanosine imino peak of bp 3 is 14.5 Hz). The Mn^{2+} binding as monitored by NMR was not dependent on the presence of the ACCA end.

Though the Mn^{2+} concentration was 150–200 times lower than the RNA concentration, Mn^{2+} was obviously able to influence all of the RNA duplexes, suggesting a fast exchange of the ions between RNA and the solvent. Nevertheless, Mn^{2+} preferentially occupied certain sites on the RNA that

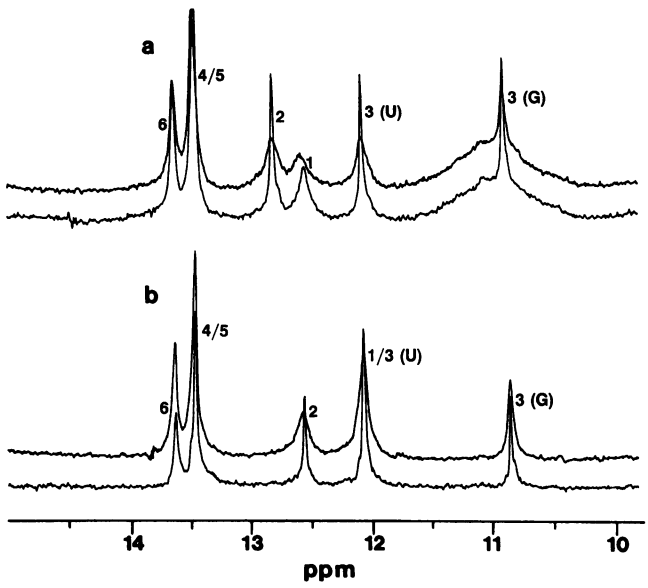

FIG. 5. Effect of the addition of Mn^{2+} on the imino proton resonance signals at 4°C of the duplex without a dangling end (14-mer) (*a*) and the duplex with an ACCA 3′ terminus at bp 1 (18-mer) (*b*). In each case, the lower trace belongs to the solution without Mn^{2+}, and the upper trace gives the spectrum after addition of either 7.5 μM (*a*) or 5 μM (*b*) $MnCl_2$. The solutions contain 100 mM NaCl and either 7.5 mM (*a*) or 5 mM (*b*) $MgCl_2$.

were specified by the base pairs that display broadened imino resonances after addition of Mn^{2+}. The resonances of protons in the vicinity of paramagnetic probes were broadened with the excess linewidth varying as r^{-6}, where r is the distance between ion and proton (11). Hence, there is a preferred binding site for Mn^{2+} and, correspondingly, for Mg^{2+} in the vicinity of bp 2 and 3. Moreover, the imino proton line of bp 1 was broadened too, and hence, the ion binding site should lie within a radius of not more than ≈10 Å from that imino proton.

Addition of $MnCl_2$ to duplexes with an I·U, I·C, and G·C base pair at position 3 did not cause significant alterations in the imino regions of the corresponding proton NMR spectra (data not shown). This observation was not dependent on the presence of the 3′-ACCA end. Moreover, similar studies with acceptor stem microhelices derived from *E. coli* $tRNA^{Gly}$ and $tRNA^{His}$ (13) likewise did not reveal any distinct and specific line broadening, indicating that there are no specific Mn^{2+} binding sites (data not shown).

DISCUSSION

Influence of Dangling 3′ Ends. The acceptor stem of the $tRNA^{Ala}$ from *E. coli* has evolved as a stable RNA helix, permitting the incorporation of a unique recognition element provided by the G·U pair at position 3. In particular, the combination of the first G1·C72 base pair of the stem and the first nonpaired (discriminator) base A73 lends high stability to the duplex, especially to its first and second base pairs. The unpaired single-stranded 3′ nucleotides seem to be stacked fairly regularly, possibly by the continuation of the helix. Though a single dangling 3′ adenosine contributes the major portion (−7.6 kJ/mol) of the total stability increase, the effect of the other bases is still clearly observable. The contribution of the CCA end to the stability of the aminoacyl region of tRNA is still −2.9 kJ/mol.

Stacking the ACCA end upon the aminoacyl stem can be predicted from the systematic up-field shifts of the imino resonances of bp 1 and 2 after stepwise extension of the 3′ end. The up-field shifts for imino protons in base pairs, induced by the base ring currents of the regularly stacked nearest- and next-nearest-neighbor base pairs, respectively, can be approximately calculated (14, 15). The values obtained in this way are strictly valid only for a rigid canonical A-form helix. The experimentally observed up-field shifts are distinctly smaller than the predicted ones for the first base pair, whereas they are much greater than the theoretical values for the second base pair. Although there should be no up-field shifts for bases being spaced by >1 nt in the sequence, as can be seen from Fig. 4, even the influence of the third nucleotide in the single-stranded terminus is sensed by bp 2. This cannot be explained by a direct interaction of the nonpaired base via ring current effects. Probably, it is mediated by a successive ordering of the bases above the helical stem. The stepwise addition of unpaired 3′ bases increasingly reduces the conformational mobility and enhances the stacking order. As a result the stability of the bp 1 is particularly increased.

Effects of Sequence Variations. If the G·U pair at position 3 is replaced by an I·U pair in both the 14-mer and the 18-mer, the ΔG^0 and T_m are markedly reduced (cf., Tables 1 and 2) though the stacking properties of guanosine and inosine are comparable (16). This implies that the 2-amino group of guanine, which projects into the minor groove of the RNA double helix, is important for the stability of the duplex. Since in the G·U pair the 2-amino group is not involved in hydrogen bonding between the paired bases, this is probably brought about by an interaction with other functional groups.

By crystal structure analysis of a G·U pair-containing RNA duplex (17), a water-mediated interaction of the guanosine 2′-hydroxyl and 2-amino groups was suggested. In this study by using proton NMR, we demonstrate the existence of a specific metal ion binding site in the vicinity of bp 2 and 3. No such binding site was found when G·U pair at position 3 was replaced by other base pairs. Since the G3·U70 base pair is crucial for the recognition of corresponding microhelices by Ala-tRNA synthetase (18), an involvement of a metal ion binding site in this process seems possible.

In summary, for the recognition of *E. coli* $tRNA^{Ala}$ by its cognate tRNA synthetase, a relatively stable helical stem, continued by a similarly ordered possibly helical single-stranded end, seems to be necessary in addition to the crucially important G·U pair at position 3.

The first base pair G1·C72 and discriminator base A73 of many tRNA acceptor stems are combined to give high duplex stability. As demonstrated in this work, the nature of the discriminator base 73 exerts a strong influence on structure and stability of the acceptor stem. Thus, the discriminator base can, at least in some cases, form an "accessory" identity element that is acting indirectly via its influence on the structure and stability of the acceptor stem.

For the acceptor stem of $tRNA^{Gln}$ from *E. coli*, the 3′-ACCG terminus is attached to the adenosine of an A·U pair. This A·U base pair has to be "melted" on binding to the Gln-tRNA synthetase (19). This combination is comparable in sequence and stability to the duplex investigated in this work with a 3′-ACCA terminus at the A·U base pair at position 7, which is marked by its extraordinarily low stability.

We thank Dr. M. Yarus and M. D. Welch for comments and suggestions. This research was supported by the Deutsche Forschungsgemeinschaft, Sonderforschungsbereich 213 (project D4), and the Fonds der Chemischen Industrie.

1. Crothers, D. M., Seno, T. & Söll, D. G. (1972) *Proc. Natl. Acad. Sci. USA* **69**, 3063–3067.
2. Sprinzl, M., Dank, N., Nock, S. & Schön, A. (1991) *Nucleic Acids Res.* **19**, Suppl., 2127–2171.
3. Turner, D. H., Sugimoto, N. & Freier, S. M. (1988) *Annu. Rev. Biophys. Biophys. Chem.* **17**, 167–192.
4. Freier, S. M., Kierzek, R., Jaeger, J. A., Sugimoto, N., Caruthers, M. H., Neilson, T. & Turner, D. H. (1986) *Proc. Natl. Acad. Sci. USA* **83**, 9373–9377.
5. Francklyn, C. & Schimmel, P. (1989) *Nature (London)* **337**, 478–481.
6. Musier-Forsyth, K., Scaringe, S., Usman, N. & Schimmel, P. (1991) *Proc. Natl. Acad. Sci. USA* **88**, 209–213.
7. Teeter, M. M., Quigley, G. J. & Rich, A. (1980) in *Nucleic Acid–Metal Ion Interaction*, ed. Spiro, T. G. (Wiley, New York), pp. 145–177.
8. Arnold, L., Smrt, J., Zajicek, J., Ott, G., Schieβwohl, M. & Sprinzl, M. (1991) *Collect. Czech. Chem. Commun.* **56**, 1948–1956.
9. Hore, P. J. (1983) *J. Magn. Reson.* **54**, 539–542.
10. Puglisi, J. D. & Tinoco, I., Jr. (1989) *Methods Enzymol.* **180**, 304–325.
11. Craik, D. J. & Higgins, K. A. (1989) *Annu. Rep. Nucl. Magn. Reson. Spectrosc.* **22**, 61–138.
12. Schreier, A. A. & Schimmel, P. (1974) *J. Mol. Biol.* **86**, 601–620.
13. Francklyn, C., Shi, J.-P. & Schimmel, P. (1992) *Science* **255**, 1121–1125.
14. Arter, D. B. & Schmidt, P. G. (1976) *Nucleic Acids Res.* **3**, 1437–1447.
15. Giessner-Prettre, C., Pullman, B. & Caillet, J. (1977) *Nucleic Acids Res.* **4**, 99–116.
16. Turner, D. H., Sugimoto, N., Kierzek, R. & Dreiker, S. D. (1987) *J. Am. Chem. Soc.* **109**, 3783–3785.
17. Holbrook, S. R., Cheong, C., Tinoco, I., Jr., & Kim, S.-H. (1991) *Nature (London)* **353**, 579–581.
18. Musier-Forsyth, K., Usman, N., Scaringe, S., Doudna, J., Green, R. & Schimmel, P. (1991) *Science* **253**, 784–786.
19. Rould, M. A., Perona, J. J., Söll, D. & Steitz, T. A. (1989) *Science* **246**, 1135–1142.